

Global analysis of electroweak data in the Standard Model

J. de Blas,¹ M. Ciuchini,² E. Franco,³ A. Goncalves,⁴ S. Mishima,⁵ M. Pierini,⁶ L. Reina,⁴ and L. Silvestrini³

¹*CAFPE and Departamento de Física Teórica y del Cosmos,*

Universidad de Granada, Campus de Fuentenueva, E-18071 Granada, Spain

²*INFN, Sezione di Roma Tre, Via della Vasca Navale 84, I-00146 Roma, Italy*

³*INFN, Sezione di Roma, Piazzale A. Moro 2, I-00185 Roma, Italy*

⁴*Physics Department, Florida State University,*

Tallahassee, FL 32306-4350, USA

⁵*Theory Center, IPNS, KEK, Tsukuba 305-0801, Japan*

⁶*CERN, 1211 Geneva 23, Switzerland*

We perform a global fit of electroweak data within the Standard Model, using state-of-the-art experimental and theoretical results, including a determination of the electromagnetic coupling at the electroweak scale based on recent lattice calculations. In addition to the posteriors for all parameters and observables obtained from the global fit, we present indirect determinations for all parameters and predictions for all observables. Furthermore, we present full predictions, obtained using only the experimental information on Standard Model parameters, and a fully indirect determination of Standard Model parameters using only experimental information on electroweak data. Finally, we discuss in detail the compatibility of experimental data with the Standard Model and find a global p -value of 0.5.

In the Standard Model (SM) of ElectroWeak (EW) and strong interactions, the $SU(2)_L \otimes U(1)_Y$ gauge symmetry is hidden at low energies through the Higgs mechanism, leaving only electromagnetism as a manifest symmetry. This hidden symmetry endows the SM with calculable relations among masses and couplings of EW bosons, and a huge theoretical effort in multi-loop calculations has led to the reduction of theoretical errors in these relations down to $\mathcal{O}(10^{-4} - 10^{-5})$ [1–31]. On the experimental side, the monumental legacy of on- and off-peak measurements of EW boson masses and couplings in e^+e^- collisions at SLD, LEP, and LEP2 [32, 33] has been supplemented by TeVatron results [34–36] and is being further improved at the LHC [37–47]. The discovery of the Higgs boson [48] completed the SM Lagrangian and marked a change of perspective in the study of EW Precision Data (EWPD), allowing to fully exploit their constraining power: all observables in the EW sector can be precisely predicted, the overall consistency of the fit can be assessed and SM parameters can be indirectly determined from the fit. We carry out this program in a Bayesian framework, using state-of-the-art experimental and theoretical results.

The study presented in this paper is carried out using the `HEPfit` package [49, 50], a software tool to combine direct and indirect constraints on the Standard Model and its extensions.¹ We perform a Bayesian fit using the `HEPfit` Markov Chain Monte Carlo (MCMC) engine based on the `BAT` library [51].

The list of parameters and EW precision observables (EWPO) included in our study is shown in Tables I and II, where we present results for the SM fit of EWPD both in a *standard* (Table I) and in a *conservative* (Table II) scenario, depending on the assumptions made in combining different measurements of m_t and m_H , as described below.

The main framework of the EW fit as implemented in `HEPfit` can be found in Refs. [52, 53], to which we refer the reader for a more detailed description of how various EWPO have been implemented, and for a complete account of the literature on which such implementations are based. With respect to our previous studies, we now also take into account the latest developments on the theory side, such as the recent calculation of the 2-loop EW bosonic corrections to $\sin^2 \theta_{\text{eff}}^b$ [30], as well as the full 2-loop corrections to the partial decays of the Z from Ref. [31]. As explained in Ref. [31], such corrections are very small and indeed we find they have no noticeable effect on the fit results.²

Among the input parameters, G_μ and $\alpha(0)$ are fixed ($G_\mu = 1.1663787 \times 10^{-5} \text{ GeV}^{-2}$ and $\alpha(0) = 1/137.035999139$ [56]), while $\alpha_s(M_Z^2)$, $\Delta\alpha_{\text{had}}^{(5)}(M_Z^2)$, M_Z , m_t , and m_H are varied in the MCMC process. Compared to our latest analysis [53], the EW fit presented in this paper contains several updates that are summarized below:³

1. The value of the strong coupling constant at the Z pole has been updated with the last average from the Particle Data Group (PDG), $\alpha_s(M_Z^2) = 0.1179 \pm 0.0010$ [58]. To avoid double counting the experimental information on EW observables, we exclude from this combination the indirect determination from the EW fit and obtain $\alpha_s(M_Z^2) = 0.1177 \pm 0.0010$. This updates the previous average used in Ref. [53], $\alpha_s(M_Z^2) = 0.1179 \pm 0.0012$. The small differences, both in the central value and error, have only a small effect on the global EW fit.

¹ The `HEPfit` package is available under the GNU General Public License (GPL) [50].

² The recent evaluation of the leading fermionic three-loop corrections to EWPO [54, 55] results in even smaller effects, which have been neglected in our fits.

³ For recent comprehensive reviews of both theoretical and experimental inputs to EW precision fits see Ref. [56] and Ref. [57].

Global SM EW fit (<i>standard</i> scenario)					
	Measurement	Posterior	Prediction	1D Pull	nD Pull
$\alpha_s(M_Z^2)$	0.1177 ± 0.0010	0.11792 ± 0.00094 [0.11606, 0.11978]	0.1198 ± 0.0028 [0.1143, 0.1253]	-0.7	
$\Delta\alpha_{\text{had}}^{(5)}(M_Z^2)$	0.02766 ± 0.00010	0.027627 ± 0.000096 [0.027436, 0.027815]	0.02717 ± 0.00037 [0.02646, 0.02789]	1.3	
M_Z [GeV]	91.1875 ± 0.0021	91.1883 ± 0.0021 [91.1842, 91.1922]	91.2047 ± 0.0088 [91.1874, 91.2217]	-1.9	
m_t [GeV]	172.58 ± 0.45	172.75 ± 0.44 [171.89, 173.62]	176.2 ± 2.0 [172.2, 180.0]	-1.8	
m_H [GeV]	125.21 ± 0.12	125.21 ± 0.12 [124.97, 125.44]	108.3 ± 11.7 [90.1, 137.4]	1.3	
M_W [GeV]	80.379 ± 0.012	80.3591 ± 0.0052 [80.3489, 80.3692]	80.3545 ± 0.0057 [80.3433, 80.3659]	1.8	
Γ_W [GeV]	2.085 ± 0.042	2.08827 ± 0.00055 [2.08719, 2.08936]	2.08829 ± 0.00056 [2.08720, 2.08938]	-0.1	
$\sin^2 \theta_{\text{eff}}^{\text{lept}}(Q_{\text{FB}}^{\text{had}})$	0.2324 ± 0.0012	0.231509 ± 0.000056 [0.231399, 0.231619]	0.231511 ± 0.000058 [0.231398, 0.231623]	0.7	
$P_\tau^{\text{pol}} = \mathcal{A}_\ell$	0.1465 ± 0.0033	0.14712 ± 0.00044 [0.14625, 0.14799]	0.14713 ± 0.00045 [0.14626, 0.14801]	-0.2	
Γ_Z [GeV]	2.4955 ± 0.0023	2.49443 ± 0.00065 [2.49317, 2.49569]	2.49423 ± 0.00069 [2.49289, 2.49558]	0.5	
σ_h^0 [nb]	41.480 ± 0.033	41.4908 ± 0.0076 [41.4756, 41.5057]	41.4927 ± 0.0079 [41.4772, 41.5086]	-0.4	
R_ℓ^0	20.767 ± 0.025	20.7493 ± 0.0080 [20.7337, 20.7651]	20.7462 ± 0.0087 [20.7291, 20.7632]	0.8	1.0
$A_{\text{FB}}^{0,\ell}$	0.0171 ± 0.0010	0.016234 ± 0.000098 [0.016043, 0.016425]	0.016225 ± 0.000097 [0.016035, 0.016417]	0.9	
\mathcal{A}_ℓ (SLD)	0.1513 ± 0.0021	0.14712 ± 0.00044 [0.14625, 0.14799]	0.14713 ± 0.00046 [0.14622, 0.14803]	1.9	
R_b^0	0.21629 ± 0.00066	0.215878 ± 0.000100 [0.215681, 0.216075]	0.21587 ± 0.00010 [0.21567, 0.21607]	0.6	
R_c^0	0.1721 ± 0.0030	0.172205 ± 0.000054 [0.172100, 0.172310]	0.172206 ± 0.000053 [0.172101, 0.172311]	0.0	
$A_{\text{FB}}^{0,b}$	0.0996 ± 0.0016	0.10314 ± 0.00031 [0.10253, 0.10375]	0.10315 ± 0.00033 [0.10251, 0.10378]	-2.2	1.3
$A_{\text{FB}}^{0,c}$	0.0707 ± 0.0035	0.07369 ± 0.00023 [0.07324, 0.07414]	0.07370 ± 0.00024 [0.07322, 0.07416]	-0.9	
\mathcal{A}_b	0.923 ± 0.020	0.934738 ± 0.000040 [0.934661, 0.934817]	0.934739 ± 0.000040 [0.934661, 0.934818]	-0.6	
\mathcal{A}_c	0.670 ± 0.027	0.66782 ± 0.00022 [0.66739, 0.66825]	0.66783 ± 0.00022 [0.66740, 0.66825]	0.0	
\mathcal{A}_s	0.895 ± 0.091	0.935651 ± 0.000040 [0.935573, 0.935730]	0.935651 ± 0.000040 [0.935572, 0.935729]	-0.4	
$\text{BR}_{W \rightarrow \ell \bar{\nu}_\ell}$	0.10860 ± 0.00090	0.108381 ± 0.000022 [0.108337, 0.108424]	0.108380 ± 0.000022 [0.108337, 0.108423]	0.2	
$\sin^2 \theta_{\text{eff}}^{\text{lept}}$ (HC)	0.23143 ± 0.00025	0.231509 ± 0.000056 [0.231399, 0.231619]	0.231511 ± 0.000058 [0.231398, 0.231623]	-0.3	
R_{uc}	0.1660 ± 0.0090	0.172227 ± 0.000032 [0.172166, 0.172290]	0.172228 ± 0.000032 [0.172166, 0.172290]	-0.7	

TABLE I. Experimental measurement, result of the global fit, prediction, and pull for the five input parameters ($\alpha_s(M_Z^2)$, $\Delta\alpha_{\text{had}}^{(5)}(M_Z^2)$, M_Z , m_t , m_H), and for the set of EWPO considered in the fit, in the *standard* scenario for m_t and m_H . For the results of the global fit and for the predictions, the 95% probability range is reported in square brackets. The values in the column *Prediction* are determined without using the corresponding experimental information. Pulls are calculated both as individual pulls (*1D Pull*) and as global pulls (*nD Pull*) for sets of correlated observables, and are given in units of standard deviations. Groups of correlated observables are identified by shades of grey.

Global SM EW fit (<i>conservative</i> scenario)					
	Measurement	Posterior	Prediction	1D Pull	nD Pull
$\alpha_s(M_Z^2)$	0.1177 ± 0.0010	0.11793 ± 0.00094 [0.11610, 0.11979]	0.1199 ± 0.0028 [0.1143, 0.1254]	-0.7	
$\Delta\alpha_{\text{had}}^{(5)}(M_Z^2)$	0.02766 ± 0.00010	0.027631 ± 0.000097 [0.027441, 0.027823]	0.02721 ± 0.00039 [0.02646, 0.02797]	1.1	
M_Z [GeV]	91.1875 ± 0.0021	91.1881 ± 0.0021 [91.1841, 91.1922]	91.2045 ± 0.0094 [91.1859, 91.2231]	-1.8	
m_t [GeV]	172.6 ± 1.0	173.31 ± 0.90 [171.55, 175.06]	176.1 ± 2.0 [172.2, 180.0]	-1.6	
m_H [GeV]	125.21 ± 0.21	125.21 ± 0.21 [124.80, 125.62]	109.7 ± 12.6 [89.9, 141.2]	1.2	
M_W [GeV]	80.379 ± 0.012	80.3619 ± 0.0064 [80.3491, 80.3746]	80.3549 ± 0.0077 [80.3398, 80.3700]	1.7	
Γ_W [GeV]	2.085 ± 0.042	2.08850 ± 0.00063 [2.08725, 2.08974]	2.08849 ± 0.00063 [2.08726, 2.08975]	-0.1	
$\sin^2 \theta_{\text{eff}}^{\text{lept}}(Q_{\text{FB}}^{\text{had}})$	0.2324 ± 0.0012	0.231497 ± 0.000058 [0.231382, 0.231612]	0.231498 ± 0.000060 [0.231380, 0.231617]	0.8	
$P_{\tau}^{\text{pol}} = \mathcal{A}_{\ell}$	0.1465 ± 0.0033	0.14722 ± 0.00046 [0.14632, 0.14813]	0.14724 ± 0.00046 [0.14632, 0.14814]	-0.2	
Γ_Z [GeV]	2.4955 ± 0.0023	2.49454 ± 0.00066 [2.49323, 2.49584]	2.49434 ± 0.00070 [2.49297, 2.49573]	0.5	
σ_h^0 [nb]	41.480 ± 0.033	41.4912 ± 0.0077 [41.4761, 41.5062]	41.4931 ± 0.0080 [41.4774, 41.5091]	-0.4	
R_{ℓ}^0	20.767 ± 0.025	20.7492 ± 0.0080 [20.7335, 20.7650]	20.7458 ± 0.0087 [20.7290, 20.7629]	0.8	0.9
$A_{\text{FB}}^{0,\ell}$	0.0171 ± 0.0010	0.01626 ± 0.00010 [0.01606, 0.01645]	0.01625 ± 0.00010 [0.01605, 0.01645]	0.9	
\mathcal{A}_{ℓ} (SLD)	0.1513 ± 0.0021	0.14722 ± 0.00046 [0.14632, 0.14813]	0.14724 ± 0.00048 [0.14629, 0.14819]	1.9	
R_b^0	0.21629 ± 0.00066	0.21586 ± 0.00010 [0.21565, 0.21606]	0.21585 ± 0.00010 [0.21564, 0.21606]	0.7	
R_c^0	0.1721 ± 0.0030	0.172212 ± 0.000055 [0.172106, 0.172318]	0.172212 ± 0.000054 [0.172106, 0.172319]	0.0	
$A_{\text{FB}}^{0,b}$	0.0996 ± 0.0016	0.10321 ± 0.00033 [0.10257, 0.10384]	0.10323 ± 0.00034 [0.10255, 0.10389]	-2.2	1.3
$A_{\text{FB}}^{0,c}$	0.0707 ± 0.0035	0.07374 ± 0.00024 [0.07326, 0.07422]	0.07375 ± 0.00025 [0.07325, 0.07425]	-0.9	
\mathcal{A}_b	0.923 ± 0.020	0.934741 ± 0.000040 [0.934662, 0.934819]	0.934741 ± 0.000040 [0.934662, 0.934820]	-0.6	
\mathcal{A}_c	0.670 ± 0.027	0.66787 ± 0.00023 [0.66742, 0.66832]	0.66788 ± 0.00023 [0.66742, 0.66833]	0.1	
\mathcal{A}_s	0.895 ± 0.091	0.935660 ± 0.000042 [0.935577, 0.935743]	0.935659 ± 0.000042 [0.935578, 0.935742]	-0.4	
$\text{BR}_{W \rightarrow \ell \bar{\nu}_{\ell}}$	0.10860 ± 0.00090	0.108380 ± 0.000022 [0.108337, 0.108424]	0.108380 ± 0.000022 [0.108337, 0.108424]	0.2	
$\sin^2 \theta_{\text{eff}}^{\text{lept}}(\text{HC})$	0.23143 ± 0.00025	0.231497 ± 0.000058 [0.231382, 0.231612]	0.231498 ± 0.000060 [0.231380, 0.231617]	-0.3	
R_{uc}	0.1660 ± 0.0090	0.172234 ± 0.000033 [0.172170, 0.172299]	0.172234 ± 0.000033 [0.172170, 0.172299]	-0.7	

TABLE II. Same as Table I in the *conservative* scenario for the errors on m_t and m_H .

2. The value for the five-flavour hadronic contribution to the QED coupling constant at the Z -boson mass has also been recently updated by several groups, with mostly compatible results (see Ref. [57] for a more comprehensive discussion). In our study we make use of the lattice determinations of the euclidean correlation function $\hat{\Pi}_{n_f=4}(-4\text{GeV}^2) = 0.0712 \pm 0.0002$ from Ref. [59] (Table S3) and of the bottom quark contribution $\hat{\Pi}_b(-4\text{GeV}^2) = 0.00013$ from Ref. [60], which combined give

$$\Delta\alpha_{\text{had}}^{(5)}(-4\text{GeV}^2) = 4\pi\alpha \left(\hat{\Pi}_{n_f=4}(-4\text{GeV}^2) + \hat{\Pi}_b(-4\text{GeV}^2) \right) = 0.00654 \pm 0.00002.$$

Running perturbatively to the scale $-M_Z^2$ and continuing analytically to Minkowski spacetime according to Ref. [61] leads to $\Delta\alpha_{\text{had}}^{(5)}(M_Z^2) = 0.02766 \pm 0.00010$, compatible with, but more precise than, the value we previously used [53], $\Delta\alpha_{\text{had}}^{(5)}(M_Z^2) = 0.02750 \pm 0.00033$.

3. For the top-quark mass, Ref. [53] used the 2014 world average from ATLAS and the Tevatron experiments. Since then several updated measurements have become available, with individual uncertainties exceeding that of the 2014 average. We have therefore reconsidered and updated the value of and uncertainty on m_t that is used on the current EW precision fit. In this study we consider: i) the 2016 Tevatron [62] combination; ii) the 2015 CMS Run 1 combination [37]; iii) the combination of ATLAS Run 1 results in Ref. [38]; iii) the CMS Run 2 measurements in the dilepton, lepton+jets and all-jet channels [39–41]; and iv) the ATLAS Run 2 result from the lepton+jet channel [42]. Unfortunately, combining these different measurements is non-trivial due to the correlations between theoretical errors and several of the systematic uncertainties of the different measurements. For the purpose of this paper, we consider a correlated combination between the different measurements,⁴ assuming the linear correlation coefficient between two systematic uncertainties to be written as $\rho_{ij}^{\text{sys}} = \min\{\sigma_i^{\text{sys}}, \sigma_j^{\text{sys}}\} / \max\{\sigma_i^{\text{sys}}, \sigma_j^{\text{sys}}\}$. This results in $m_t = 172.58 \pm 0.45$ GeV. In performing this combination, we note that, while the LHC measurements of m_t are reasonably consistent with each other, there is some tension between the ATLAS and CMS lepton+jet values. This is also the case between the LHC and Tevatron m_t combinations, and while these tensions could be just due to statistical fluctuations, in the worst case scenario they could indicate that some of the systematics included in these measurements have been underestimated. A common way of dealing with this issue is to use a rescaled error following the PDG average method [58]. In our case the resulting uncertainty would turn out to be unreasonably large, ~ 1.7 GeV. For the purpose of this paper we illustrate the impact of the top-mass uncertainty on the SM precision fits by considering two scenarios: one where we use the *standard* error of $\delta m_t = 0.45$ GeV and one where we consider a more *conservative* error of $\delta m_t = 1$ GeV. As we will see, the two different scenarios lead at the moment to very similar results since the parametric uncertainties are subleading with respect to the experimental ones.
4. The Higgs-boson mass, whose value after Run 1 was $m_H = 125.09 \pm 0.24$ GeV [48] (as used in Ref. [53]), has now also been measured in Run 2 both by ATLAS [64, 65] and CMS [66, 67] in the 4ℓ and $\gamma\gamma$ channels. We follow the same combination procedure as for m_t and combine all the different measurements to obtain $m_H = 125.21 \pm 0.12$ GeV as the *standard* input value for our fits. Some tension between the ATLAS and CMS Run 2 combinations is also present in this case. This tension does not have a visible impact in the fits, since the parametric uncertainty associated to m_H is negligible for δm_H up to $\mathcal{O}(10)$ GeV. Nevertheless, we consider an uncertainty $\delta m_H = 0.21$ GeV for the *conservative* scenario, obtained using the PDG scaling method [58].
5. The ATLAS collaboration presented their first direct determination of the W -boson mass, $M_W = 80.370 \pm 0.019$ GeV [43], with an uncertainty comparable to the current LEP2+Tevatron average. Assuming the absence of significant correlations between the LHC and Tevatron determinations, one can compute an approximate “world average” of $M_W = 80.379 \pm 0.012$ GeV. Although different from the LEP2+Tevatron world average used in Ref. [53], $M_W = 80.385 \pm 0.015$ GeV, the update of M_W has a very minor effect on the SM fits.⁵
6. The determination of the effective leptonic weak mixing angle, $\sin^2 \theta_{\text{eff}}^{\text{lept}}$, at hadron colliders has also been updated. Using the same procedure as for the Higgs-boson and top-quark masses, we combine the ATLAS [44, 45] and CMS [46] measurements, the Tevatron determinations in Ref. [69], and the LHCb measurement in Ref. [47]. This combination is done separately for the measurements in the electron and muon channels, yielding $\sin^2 \theta_{\text{eff}}^{ee} = 0.23175 \pm 0.00029$ and $\sin^2 \theta_{\text{eff}}^{\mu\mu} = 0.23093 \pm 0.00039$, respectively. We also obtain a combination assuming lepton universality, $\sin^2 \theta_{\text{eff}}^{\text{lept}} = 0.23143 \pm 0.00025$. In this last case, we note that there is some tension between the CDF and D0 values, but this would only result in a small rescaling of the error and it is ignored here.

⁴ We do not consider the CMS measurement using the single-top channel [63], but we checked it has a negligible impact on the average.

⁵ The very recent result on M_W from the LHCb Collaboration [68] will be included in future updates of our fit.

	Prediction				<i>standard</i> scenario		<i>conservative</i> scenario	
		$\alpha_s(M_Z^2)$	$\Delta\alpha_{\text{had}}^{(5)}(M_Z^2)$	M_Z	m_t	Total	m_t	Total
M_W [GeV]	80.3545	± 0.0006	± 0.0018	± 0.0027	± 0.0027	± 0.0042	± 0.0060	± 0.0069
Γ_W [GeV]	2.08782	± 0.00040	± 0.00014	± 0.00021	± 0.00021	± 0.00052	± 0.00047	± 0.00066
Γ_Z [GeV]	2.49414	± 0.00049	± 0.00010	± 0.00021	± 0.00010	± 0.00056	± 0.00023	± 0.00060
σ_h^0 [nb]	41.4929	± 0.0049	± 0.0001	± 0.0020	± 0.0003	± 0.0053	± 0.0007	± 0.0053
$\sin^2 \theta_{\text{eff}}^{\text{lept}}$	0.231534	± 0.000003	± 0.000035	± 0.000015	± 0.000013	± 0.000041	± 0.000030	± 0.000048
\mathcal{A}_ℓ	0.14692	± 0.00003	± 0.00028	± 0.00012	± 0.00010	± 0.00032	± 0.00023	± 0.00038
\mathcal{A}_c	0.66775	± 0.00001	± 0.00012	± 0.00005	± 0.00005	± 0.00014	± 0.00011	± 0.00017
\mathcal{A}_b	0.934727	± 0.000001	± 0.000023	± 0.000010	± 0.000003	± 0.000025	± 0.000007	± 0.000026
$A_{\text{FB}}^{0,\ell}$	0.016191	± 0.000006	± 0.000060	± 0.000026	± 0.000023	± 0.000070	± 0.000052	± 0.000084
$A_{\text{FB}}^{0,c}$	0.07358	± 0.00001	± 0.00015	± 0.00006	± 0.00006	± 0.00018	± 0.00013	± 0.00021
$A_{\text{FB}}^{0,b}$	0.10300	± 0.00002	± 0.00020	± 0.00008	± 0.00007	± 0.00023	± 0.00016	± 0.00027
R_ℓ^0	20.7464	± 0.0062	± 0.0006	± 0.0003	± 0.0002	± 0.0063	± 0.0004	± 0.0063
R_c^0	0.172198	± 0.000020	± 0.000002	± 0.000001	± 0.000005	± 0.000020	± 0.000011	± 0.000023
R_b^0	0.215880	± 0.000011	± 0.000001	± 0.000000	± 0.000015	± 0.000019	± 0.000034	± 0.000035
$\text{BR}_{W \rightarrow \ell \bar{\nu}_\ell}$	0.108386	± 0.000024	± 0.000000	± 0.000000	± 0.000000	± 0.000024	± 0.000000	± 0.000024
\mathcal{A}_s	0.935637	± 0.000002	± 0.000022	± 0.000010	± 0.000009	± 0.000026	± 0.000020	± 0.000031
R_{uc}	0.172220	± 0.000019	± 0.000002	± 0.000001	± 0.000005	± 0.000020	± 0.000011	± 0.000023

TABLE III. SM predictions computed using the theoretical expressions for the EWPO without the corresponding experimental constraints, and individual uncertainties associated with each input parameter, except for m_H (see text).

- The updates in the Z -lineshape observables reported in Ref. [70] have been included. Compared to Ref. [32], these updates are due to the use of more accurate calculations of the Bhabha cross section, which lead to a better understanding of any systematic bias on the integrated luminosity. Only the Z width, Γ_Z , the hadronic cross section at the Z peak, σ_h^0 , and its correlations with other Z -lineshape observables are noticeably affected by these updates.
- We have included the update in the determination of the forward-backward asymmetry of the bottom quark, $A_{FB}^{0,b}$, after taking into account the massive $O(\alpha_s^2)$ corrections in $e^+e^- \rightarrow b\bar{b}$ at the Z pole [71]. As we will see, these corrections slightly reduce the longstanding tension between the experimental measurement of this observable and its SM prediction.

Apart from these updates, we have also extended the EW fit by including the following extra observables:

- The determination of the s -quark asymmetry parameter \mathcal{A}_s at SLD [72].
- The PDG average of the different LEP experiment determinations of the ratio $R_{uc} \equiv \frac{1}{2}\Gamma_{Z \rightarrow u\bar{u}+c\bar{c}}/\Gamma_{Z \rightarrow \text{had}}$ [58].
- The leptonic branching ratio of the W boson, $\text{BR}_{W \rightarrow \ell \bar{\nu}_\ell} \equiv \Gamma_{W^- \rightarrow \ell^- \bar{\nu}_\ell}/\Gamma_W$ [58].

We use flat priors for all the SM input parameters, and include the information of their experimental measurements in the likelihood. We assume that all experimental distributions are Gaussian. The known *intrinsic* theoretical uncertainties due to missing higher-order corrections to EWPO are also included in the fits, using the results of Ref. [31] to which we refer for more details. The main theory uncertainties we consider are:

$$\begin{aligned} \delta_{\text{th}} M_W &= 4 \text{ MeV}, & \delta_{\text{th}} \sin^2 \theta_W &= 5 \cdot 10^{-5}, & \delta_{\text{th}} \Gamma_Z &= 0.4 \text{ MeV}, & \delta_{\text{th}} \sigma_{\text{had}}^0 &= 6 \text{ pb}, \\ \delta_{\text{th}} R_\ell^0 &= 0.006, & \delta_{\text{th}} R_c^0 &= 0.00005, & \delta_{\text{th}} R_b^0 &= 0.0001. \end{aligned} \quad (1)$$

These uncertainties are implemented in the fit as nuisance parameters with Gaussian prior distributions. Theoretical uncertainties are still small compared to the experimental ones and, therefore, they have a very small impact on the fit. The same applies to the *parametric* theory uncertainties, obtained by propagating the experimental errors of the SM inputs into the predictions for the EWPO. The breakdown of these parametric errors is detailed in Table III, except for the contributions coming from the uncertainty in m_H , which, even in the conservative scenario, are numerically irrelevant in the total parametric uncertainty.

For each observable, we give in Tables I and II, the experimental information used as input (*Measurement*), together with the output of the combined fit (*Posterior*), and the *Prediction* of the same quantity. The latter is obtained from the posterior predictive distribution derived from a combined analysis of all the other quantities. The compatibility of the constraints is then evaluated by sampling the posterior predictive distribution and the experimental one, by

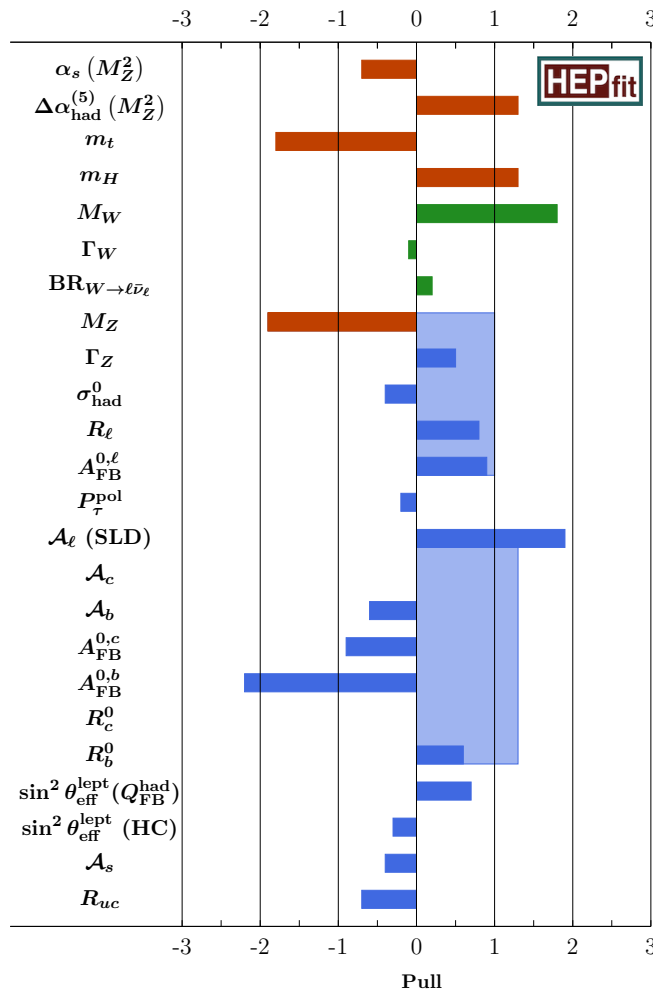


FIG. 1. 1D pulls between the observed experimental values and the SM predictions (indirect determinations) for the different EWPO (SM input parameters) considered in the fit, for the *standard* scenario. (The different colors in the figure are simply used to distinguish the SM inputs [orange], charged-current observables [green] and neutral-current observables [blue].) Each prediction is obtained removing the corresponding observable from the fit. The *transparent* bars represent the corresponding nD pulls for groups of correlated observables. See text for details.

constructing the probability density function (p.d.f.) of the residuals $p(x)$, and by computing the integral of the p.d.f. in the region $p(x) < p(0)$. This two-sided p -value is then converted to the equivalent number of standard deviations for a Gaussian distribution. In the case of a Gaussian posterior predictive distribution, this quantity coincides with the usual pull defined as the difference between the central values of the two distributions divided by the sum in quadrature of the residual mean square of the distributions themselves. The advantage of this approach is that no approximation is made on the shape of p.d.f.'s. These *1D pulls* are also shown in Figure 1. We can see a clear consistency between the measurement of all EWPO and their SM predictions. Only $A_{\text{FB}}^{0,b}$ shows some tension (at the 2σ level), which should be considered in investigating new physics but also treated with care given the large number of observables considered in the EW fit (see the discussion below for a quantitative assessment of the global significance taking the *look-elsewhere* effect into account).

Moreover, when interpreting this *1D pull* one needs to take into account that $A_{\text{FB}}^{0,b}$ is actually part of a set of experimentally correlated observables. In order to check the consistency between SM and experiments in this case, one can define an *nD pull* by removing from the fit one set of correlated observables at a time and computing the prediction for the set of observables together with their covariance matrix. Then the same procedure described for *1D pulls* can be carried out, this time sampling the posterior predictive and experimental n-dimensional p.d.f.'s. This *nD pull* is shown in the last column in Tables I and II, as well as in Figure 1, in which case we see that the global pull for the set of correlated observables involving $A_{\text{FB}}^{0,b}$ is reduced to 1.3σ . To get an idea of the agreement between the SM

	Measurement	Full Indirect	Pull	Full Prediction	Pull
$\alpha_s(M_Z^2)$	0.1177 ± 0.0010	0.1217 ± 0.0046	-0.8	0.1177 ± 0.0010	-
$\Delta\alpha_{\text{had}}^{(5)}(M_Z^2)$	0.02766 ± 0.00010	0.02752 ± 0.00066	0.2	0.02766 ± 0.00010	-
M_Z [GeV]	91.1875 ± 0.0021	91.200 ± 0.039	-0.3	91.1875 ± 0.0021	-
m_t [GeV]	172.58 ± 0.45	180.1 ± 9.6	-0.8	172.58 ± 0.45	-
m_H [GeV]	125.21 ± 0.12	196.2 ± 89.9	-0.4	125.21 ± 0.12	-
M_W [GeV]	80.379 ± 0.012	80.379 ± 0.012	0.0	80.3545 ± 0.0059	1.8
Γ_W [GeV]	2.085 ± 0.042	2.0916 ± 0.0023	-0.1	2.08782 ± 0.00060	-0.1
$\sin^2 \theta_{\text{eff}}^{\text{lept}}(Q_{\text{FB}}^{\text{had}})$	0.2324 ± 0.0012	0.23147 ± 0.00014	0.8	0.231534 ± 0.000062	0.7
$P_{\tau}^{\text{pol}} = \mathcal{A}_{\ell}$	0.1465 ± 0.0033	0.1474 ± 0.0011	-0.3	0.14692 ± 0.00049	-0.1
Γ_Z [GeV]	2.4955 ± 0.0023	2.4947 ± 0.0020	0.3	2.49414 ± 0.00068	0.6
σ_h^0 [nb]	41.480 ± 0.033	41.466 ± 0.031	0.3	41.4929 ± 0.0081	-0.4
R_{ℓ}^0	20.767 ± 0.025	20.765 ± 0.022	0.1	20.7464 ± 0.0086	0.8
$A_{\text{FB}}^{0,\ell}$	0.0171 ± 0.0010	0.01630 ± 0.00024	0.8	0.01619 ± 0.00011	0.9
\mathcal{A}_{ℓ} (SLD)	0.1513 ± 0.0021	0.1474 ± 0.0011	1.6	0.14692 ± 0.00049	2.0
R_b^0	0.21629 ± 0.00066	0.21562 ± 0.00035	0.9	0.21588 ± 0.00010	0.6
R_c^0	0.1721 ± 0.0030	0.17233 ± 0.00017	-0.1	0.172198 ± 0.000054	0.0
$A_{\text{FB}}^{0,b}$	0.0996 ± 0.0016	0.10334 ± 0.00077	-2.1	0.10300 ± 0.00034	-2.1
$A_{\text{FB}}^{0,c}$	0.0707 ± 0.0035	0.07386 ± 0.00059	-0.9	0.07358 ± 0.00026	-0.8
\mathcal{A}_b	0.923 ± 0.020	0.93468 ± 0.00016	-0.6	0.934727 ± 0.000041	-0.6
\mathcal{A}_c	0.670 ± 0.027	0.66805 ± 0.00048	0.1	0.66775 ± 0.00023	0.1
\mathcal{A}_s	0.895 ± 0.091	0.935693 ± 0.000088	-0.4	0.935637 ± 0.000041	-0.4
$\text{BR}_{W \rightarrow \ell \bar{\nu}_{\ell}}$	0.10860 ± 0.00090	0.10829 ± 0.00011	0.3	0.108386 ± 0.000023	0.2
$\sin^2 \theta_{\text{eff}}^{\text{lept}}(\text{HC})$	0.23143 ± 0.00025	0.23147 ± 0.00014	-0.1	0.231534 ± 0.000062	-0.4
R_{uc}	0.1660 ± 0.0090	0.17236 ± 0.00017	-0.7	0.172220 ± 0.000032	-0.7

TABLE IV. Results of the *full indirect* determination of SM parameters using only EWPD (third column) and of the *full prediction* for EWPO using only information on SM parameters (fourth column). For comparison, the input values are reported in the second column. See the text for details.

and EWPD, it is useful to consider the distribution of the p -values corresponding to the 1D pulls for the individual measurements. For purely statistical fluctuations, one expects the p -values to be uniformly distributed between 0 and 1. From the results in Tables I and II, we obtain in both scenarios an average p -value of 0.5 with $\sigma = 0.3$, fully

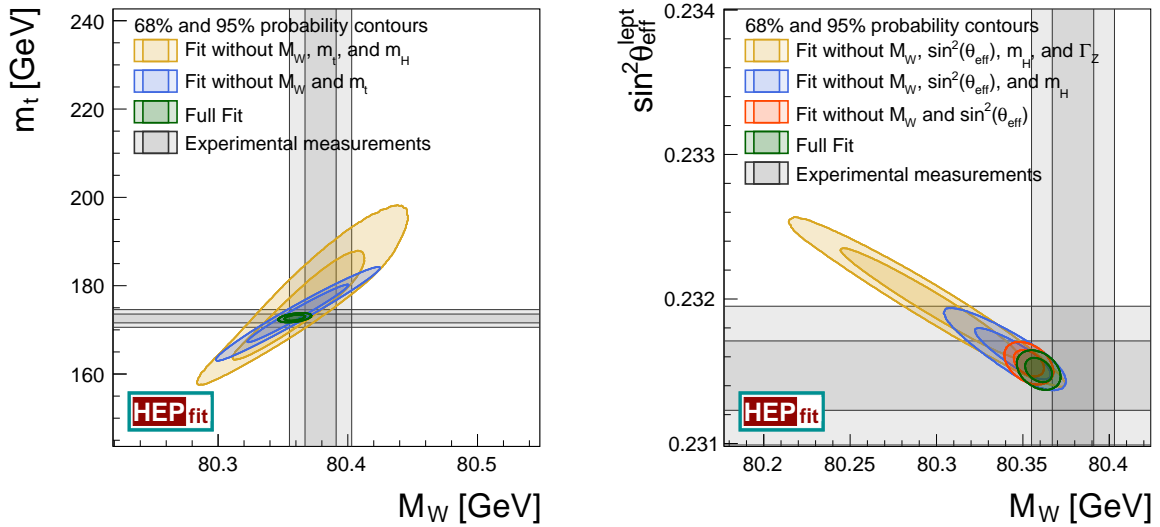


FIG. 2. Impact of various constraints in the m_t vs. M_W (left) and $\sin^2 \theta_{\text{eff}}^{\text{lept}}$ vs. M_W (right) planes. Dark (light) regions correspond to 68% (95%) probability ranges.

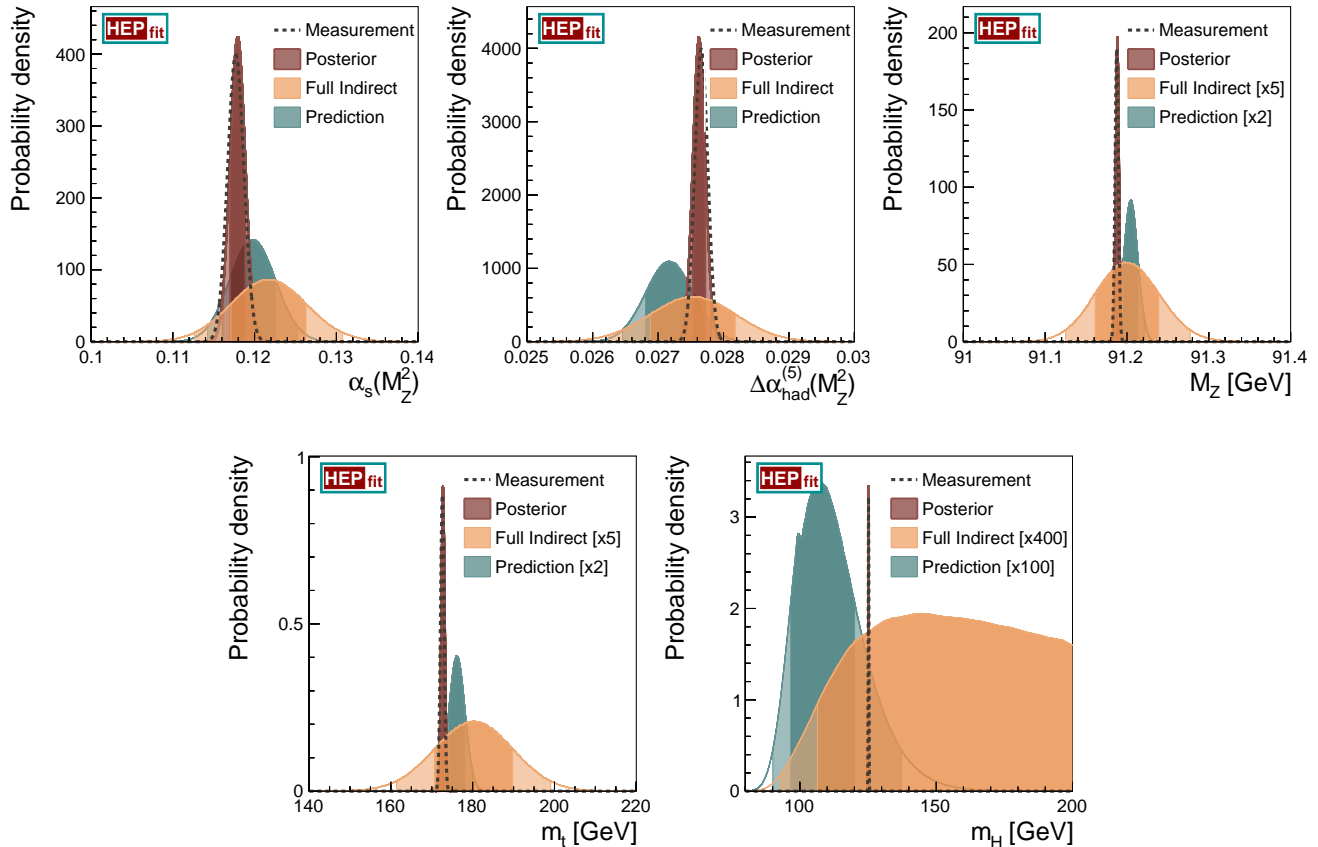


FIG. 3. Comparison among the direct measurement, the posterior, the posterior predictive (or indirect) probability distribution (denoted by "Prediction"), and the full indirect determination of the input parameters in the SM fit. The posterior predictive and the full indirect determination distributions are obtained from the fit by assuming a flat prior for the parameter under consideration or for all SM parameters respectively. To allow for a comparison with the posterior predictive distribution, the full indirect p.d.f for the Higgs mass is truncated in the figure. Dark (light) regions correspond to 68% (95%) probability ranges. `HEPfit` uses different semi-analytical approximations to the full available calculations of the EWPD, depending the range of variation of the SM inputs, see e.g. [31]. The small "bump" in the posterior predictive of the m_H figure arises as a result of the transition between these approximated expressions.

compatible with a flat distribution.

In addition to the *Predictions* obtained removing each individual observable from the fit, one can obtain a *Full Prediction* by dropping all experimental information on EWPO and just using the SM and the information on SM parameters. Conversely, one can obtain a *Full Indirect* determination of the SM parameters by dropping all information on all parameters simultaneously and determining all of them from the fit to EWPD. The results of these two extreme possibilities are reported in Table IV. Again, for the *Full Prediction* case we obtain an average p -value of 0.5 with $\sigma = 0.3$, fully compatible with a flat distribution. The results of the *Full Indirect* fit represent the best possible agreement with EWPD one could possibly reach in the SM. Indeed, in this case the tension on M_W disappears, while the tensions on \mathcal{A}_ℓ (SLD) and $A_{\text{FB}}^{0,b}$ are only mildly decreased. One would need to go beyond the SM to improve the agreement further. The tension on M_W is released by allowing for a larger value of m_t , as can be seen from the left panel of Fig. 2, where the impact of different constraints in shaping the two-dimensional p.d.f.'s of m_t vs. M_W and of $\sin^2 \theta_{\text{eff}}^{\text{lept}}$ vs. M_W is shown.

The p.d.f.'s for the SM input parameters are reported in Fig. 3, together with the posterior from the fit, the indirect determination and the *full indirect* one. While direct measurements are more precise than indirect determinations (by orders of magnitude in the case of the Higgs mass), all indirect determinations are compatible with the measurements within 2σ . Our indirect determination of $\Delta\alpha_{\text{had}}^{(5)}(M_Z^2)$ fully agrees with the independent one recently obtained in Ref. [73] using the Gfitter library [74]. The pull between the determination of $\Delta\alpha_{\text{had}}^{(5)}(M_Z^2)$ based on the BMW lattice calculation [59] and the indirect determination is of 1.3σ (1.1σ) in the *standard (conservative)* scenario, showing no

inconsistency between the current lattice evaluation and the EW fit. It will be very interesting to see if the good agreement between the lattice determination and the EW fit persists when the updated lattice value corresponding to the value of the hadronic vacuum polarization recently published in Ref. [75] is released. The indirect determination of the top mass is also compatible with the measurement at less than 2σ , but on the larger m_t side, bringing the SM further away from the Planck stability bound (see e.g. Ref. [76]).

In conclusion, EWPD appear to be fully compatible with the SM, with no more tensions than expected from statistical fluctuations. In the *standard scenario* SM fit, the largest pull neglecting correlations is 2.2σ on 24 observables, while taking correlations into account it is 1.8σ on 14 observables. In both the *full indirect* and *full prediction* determinations, the largest pull neglecting correlations is 2.1σ on 24 observables. To quantify further the agreement of the SM, we generated 600 toy experiments centered on the *full prediction* with the current experimental uncertainty and computed the fraction of toys in which the largest pull was larger than the largest one observed in real data. This fraction is an estimate of the *global p-value*. Neglecting correlations, we obtain $p = 0.53$, corresponding to 0.6σ for a Gaussian distribution, while taking into account the correlations (fixed to the values observed in current data) we get $p = 0.45$, corresponding to 0.8σ .

ACKNOWLEDGEMENTS

We thank Laurent Lellouch for informative discussions on the results of Ref. [59]. This work was supported in part by the Italian Ministry of Research (MIUR) under grant PRIN 20172LNEEZ. The work of J.B. has been supported by the FEDER/Junta de Andalucía project grant P18-FRJ-3735. The work of S.M. has been supported by the Japan Society for the Promotion of Science under grant 17K05429. The work of L.R. and A.G. has been supported by the U.S. Department of Energy under grant DE-SC0010102.

-
- [1] A. Sirlin, Radiative corrections in the $SU(2)_L \times U(1)$ theory: A simple renormalization framework, Phys.Rev. **D22**, 971 (1980).
 - [2] W. Marciano and A. Sirlin, Radiative corrections to neutrino induced neutral current phenomena in the $SU(2)_L \times U(1)$ theory, Phys.Rev. **D22**, 2695 (1980).
 - [3] A. Djouadi and C. Verzegnassi, Virtual very heavy top effects in LEP/SLC precision measurements, Phys.Lett. **B195**, 265 (1987).
 - [4] A. Djouadi, $\mathcal{O}(\alpha_s)$ vacuum polarization functions of the standard model gauge bosons, Nuovo Cim. **A100**, 357 (1988).
 - [5] B. A. Kniehl, Two-loop corrections to the vacuum polarizations in perturbative QCD, Nucl.Phys. **B347**, 86 (1990).
 - [6] F. Halzen and B. A. Kniehl, Δr beyond one loop, Nucl.Phys. **B353**, 567 (1991).
 - [7] B. A. Kniehl and A. Sirlin, Dispersion relations for vacuum polarization functions in electroweak physics, Nucl.Phys. **B371**, 141 (1992).
 - [8] B. A. Kniehl and A. Sirlin, On the effect of the $t\bar{t}$ threshold on electroweak parameters, Phys.Rev. **D47**, 883 (1993).
 - [9] R. Barbieri, M. Beccaria, P. Ciafaloni, G. Curci, and A. Vicere, Radiative correction effects of a very heavy top, Phys.Lett. **B288**, 95 (1992), arXiv:hep-ph/9205238 [hep-ph].
 - [10] R. Barbieri, M. Beccaria, P. Ciafaloni, G. Curci, and A. Vicere, Two-loop heavy top effects in the standard model, Nucl.Phys. **B409**, 105 (1993).
 - [11] A. Djouadi and P. Gambino, Electroweak gauge bosons selfenergies: Complete QCD corrections, Phys.Rev. **D49**, 3499 (1994), arXiv:hep-ph/9309298 [hep-ph].
 - [12] J. Fleischer, O. Tarasov, and F. Jegerlehner, Two-loop heavy top corrections to the ρ parameter: A simple formula valid for arbitrary Higgs mass, Phys.Lett. **B319**, 249 (1993).
 - [13] J. Fleischer, O. Tarasov, and F. Jegerlehner, Two-loop large top mass corrections to electroweak parameters: Analytic results valid for arbitrary Higgs mass, Phys.Rev. **D51**, 3820 (1995).
 - [14] L. Avdeev, J. Fleischer, S. Mikhailov, and O. Tarasov, $\mathcal{O}(\alpha_s^2)$ correction to the electroweak ρ parameter, Phys.Lett. **B336**, 560 (1994), arXiv:hep-ph/9406363 [hep-ph].
 - [15] K. Chetyrkin, J. H. Kuhn, and M. Steinhauser, Corrections of order $\mathcal{O}(G_F M_t^2 \alpha_s^2)$ to the ρ parameter, Phys.Lett. **B351**, 331 (1995), arXiv:hep-ph/9502291 [hep-ph].
 - [16] K. Chetyrkin, J. H. Kuhn, and M. Steinhauser, QCD corrections from top quark to relations between electroweak parameters to order α_s^2 , Phys.Rev.Lett. **75**, 3394 (1995), arXiv:hep-ph/9504413 [hep-ph].
 - [17] G. Degrossi, P. Gambino, and A. Vicini, Two-loop heavy top effects on the m_Z - m_W interdependence, Phys.Lett. **B383**, 219 (1996), arXiv:hep-ph/9603374 [hep-ph].
 - [18] G. Degrossi, P. Gambino, and A. Sirlin, Precise calculation of M_W , $\sin^2 \hat{\theta}_W(M_Z)$, and $\sin^2 \theta_{\text{eff}}^{\text{lep}t}$, Phys.Lett. **B394**, 188 (1997), arXiv:hep-ph/9611363 [hep-ph].
 - [19] G. Degrossi and P. Gambino, Two-loop heavy top corrections to the Z^0 boson partial widths, Nucl.Phys. **B567**, 3 (2000), arXiv:hep-ph/9905472 [hep-ph].

- [20] A. Freitas, W. Hollik, W. Walter, and G. Weiglein, Complete fermionic two-loop results for the M_W - M_Z interdependence, *Phys.Lett.* **B495**, 338 (2000), arXiv:hep-ph/0007091 [hep-ph].
- [21] J. van der Bij, K. Chetyrkin, M. Faisst, G. Jikia, and T. Seidensticker, Three-loop leading top mass contributions to the ρ parameter, *Phys.Lett.* **B498**, 156 (2001), arXiv:hep-ph/0011373 [hep-ph].
- [22] A. Freitas, W. Hollik, W. Walter, and G. Weiglein, Electroweak two-loop corrections to the M_W - M_Z mass correlation in the standard model, *Nucl.Phys.* **B632**, 189 (2002), arXiv:hep-ph/0202131 [hep-ph].
- [23] M. Awramik and M. Czakon, Complete two loop bosonic contributions to the muon lifetime in the standard model, *Phys.Rev.Lett.* **89**, 241801 (2002), arXiv:hep-ph/0208113 [hep-ph].
- [24] A. Onishchenko and O. Veretin, Two-loop bosonic electroweak corrections to the muon lifetime and M_Z - M_W interdependence, *Phys.Rev.Lett.* **B551**, 111 (2003), arXiv:hep-ph/0209010 [hep-ph].
- [25] M. Awramik, M. Czakon, A. Onishchenko, and O. Veretin, Bosonic corrections to Δr at the two loop level, *Phys.Rev.* **D68**, 053004 (2003), arXiv:hep-ph/0209084 [hep-ph].
- [26] M. Awramik and M. Czakon, Two loop electroweak bosonic corrections to the muon decay lifetime, *Nucl.Phys.Proc.Suppl.* **116**, 238 (2003), arXiv:hep-ph/0211041 [hep-ph].
- [27] M. Awramik and M. Czakon, Complete two loop electroweak contributions to the muon lifetime in the standard model, *Phys.Lett.* **B568**, 48 (2003), arXiv:hep-ph/0305248 [hep-ph].
- [28] M. Awramik, M. Czakon, A. Freitas, and G. Weiglein, Precise prediction for the W boson mass in the standard model, *Phys.Rev.* **D69**, 053006 (2004), arXiv:hep-ph/0311148 [hep-ph].
- [29] M. Faisst, J. H. Kuhn, T. Seidensticker, and O. Veretin, Three loop top quark contributions to the rho parameter, *Nucl. Phys.* **B665**, 649 (2003), arXiv:hep-ph/0302275 [hep-ph].
- [30] I. Dubovyk, A. Freitas, J. Gluza, T. Riemann, and J. Usovitsch, The two-loop electroweak bosonic corrections to $\sin^2 \theta_{\text{eff}}^b$, *Phys. Lett. B* **762**, 184 (2016), arXiv:1607.08375 [hep-ph].
- [31] I. Dubovyk, A. Freitas, J. Gluza, T. Riemann, and J. Usovitsch, Complete electroweak two-loop corrections to Z boson production and decay, *Phys. Lett. B* **783**, 86 (2018), arXiv:1804.10236 [hep-ph].
- [32] S. Schael *et al.* (ALEPH, DELPHI, L3, OPAL, SLD, LEP Electroweak Working Group, SLD Electroweak Group, SLD Heavy Flavour Group), Precision electroweak measurements on the Z resonance, *Phys. Rept.* **427**, 257 (2006), arXiv:hep-ex/0509008.
- [33] The ALEPH, DELPHI, L3, OPAL Collaborations, the LEP Electroweak Working Group, Electroweak Measurements in Electron-Positron Collisions at W-Boson-Pair Energies at LEP, *Phys. Rept.* **532**, 119 (2013), arXiv:1302.3415 [hep-ex].
- [34] ALEPH, CDF, D0, DELPHI, L3, OPAL, SLD Collaborations, LEP Electroweak Working Group, Tevatron Electroweak Working Group, and SLD Electroweak and Heavy Flavour Groups, Precision electroweak measurements and constraints on the standard model, arXiv:1012.2367 [hep-ex] (2010).
- [35] Combination of the CDF and D0 Effective Leptonic Electroweak Mixing Angles (2016).
- [36] Combination of CDF and D0 results on the mass of the top quark using up 9.7 fb^{-1} at the Tevatron, arXiv:1608.01881 [hep-ex] (2016).
- [37] V. Khachatryan *et al.* (CMS), Measurement of the top quark mass using proton-proton data at $\sqrt{s} = 7$ and 8 TeV, *Phys. Rev. D* **93**, 072004 (2016), arXiv:1509.04044 [hep-ex].
- [38] M. Aaboud *et al.* (ATLAS), Measurement of the top quark mass in the $t\bar{t} \rightarrow \text{lepton} + \text{jets}$ channel from $\sqrt{s} = 8$ TeV ATLAS data and combination with previous results, *Eur. Phys. J. C* **79**, 290 (2019), arXiv:1810.01772 [hep-ex].
- [39] A. M. Sirunyan *et al.* (CMS), Measurement of the top quark mass with lepton+jets final states using p p collisions at $\sqrt{s} = 13$ TeV, *Eur. Phys. J. C* **78**, 891 (2018), arXiv:1805.01428 [hep-ex].
- [40] A. M. Sirunyan *et al.* (CMS), Measurement of the $t\bar{t}$ production cross section, the top quark mass, and the strong coupling constant using dilepton events in pp collisions at $\sqrt{s} = 13$ TeV, *Eur. Phys. J. C* **79**, 368 (2019), arXiv:1812.10505 [hep-ex].
- [41] A. M. Sirunyan *et al.* (CMS), Measurement of the top quark mass in the all-jets final state at $\sqrt{s} = 13$ TeV and combination with the lepton+jets channel, *Eur. Phys. J. C* **79**, 313 (2019), arXiv:1812.10534 [hep-ex].
- [42] Measurement of the top quark mass using a leptonic invariant mass in pp collisions at $\sqrt{s} = 13$ TeV with the ATLAS detector (2019).
- [43] M. Aaboud *et al.* (ATLAS), Measurement of the W -boson mass in pp collisions at $\sqrt{s} = 7$ TeV with the ATLAS detector, *Eur. Phys. J. C* **78**, 110 (2018), [Erratum: *Eur.Phys.J.C* 78, 898 (2018)], arXiv:1701.07240 [hep-ex].
- [44] G. Aad *et al.* (ATLAS), Measurement of the forward-backward asymmetry of electron and muon pair-production in pp collisions at $\sqrt{s} = 7$ TeV with the ATLAS detector, *JHEP* **09**, 049, arXiv:1503.03709 [hep-ex].
- [45] Measurement of the effective leptonic weak mixing angle using electron and muon pairs from Z -boson decay in the ATLAS experiment at $\sqrt{s} = 8$ TeV (2018).
- [46] A. M. Sirunyan *et al.* (CMS), Measurement of the weak mixing angle using the forward-backward asymmetry of Drell-Yan events in pp collisions at 8 TeV, *Eur. Phys. J. C* **78**, 701 (2018), arXiv:1806.00863 [hep-ex].
- [47] R. Aaij *et al.* (LHCb), Measurement of the forward-backward asymmetry in $Z/\gamma^* \rightarrow \mu^+ \mu^-$ decays and determination of the effective weak mixing angle, *JHEP* **11**, 190, arXiv:1509.07645 [hep-ex].
- [48] G. Aad *et al.* (ATLAS, CMS), Combined Measurement of the Higgs Boson Mass in pp Collisions at $\sqrt{s} = 7$ and 8 TeV with the ATLAS and CMS Experiments, *Phys. Rev. Lett.* **114**, 191803 (2015), arXiv:1503.07589 [hep-ex].
- [49] J. de Blas *et al.*, **HEPfit**: a code for the combination of indirect and direct constraints on high energy physics models, *Eur. Phys. J. C* **80**, 456 (2020), arXiv:1910.14012 [hep-ph].
- [50] **HEPfit**: a tool to combine indirect and direct constraints on High Energy Physics, <http://hepfit.roma1.infn.it/>.

- [51] A. Caldwell, D. Kollar, and K. Kroninger, BAT: The Bayesian Analysis Toolkit, *Comput.Phys.Commun.* **180**, 2197 (2009), arXiv:0808.2552 [physics.data-an].
- [52] M. Ciuchini, E. Franco, S. Mishima, and L. Silvestrini, Electroweak Precision Observables, New Physics and the Nature of a 126 GeV Higgs Boson, *JHEP* **08**, 106, arXiv:1306.4644 [hep-ph].
- [53] J. de Blas, M. Ciuchini, E. Franco, S. Mishima, M. Pierini, L. Reina, and L. Silvestrini, Electroweak precision observables and Higgs-boson signal strengths in the Standard Model and beyond: present and future, *JHEP* **12**, 135, arXiv:1608.01509 [hep-ph].
- [54] L. Chen and A. Freitas, Leading fermionic three-loop corrections to electroweak precision observables, *JHEP* **07**, 210, arXiv:2002.05845 [hep-ph].
- [55] L. Chen and A. Freitas, Mixed EW-QCD leading fermionic three-loop corrections at $\mathcal{O}(\alpha_s\alpha^2)$ to electroweak precision observables, *JHEP* **03**, 215, arXiv:2012.08605 [hep-ph].
- [56] M. Tanabashi *et al.* (Particle Data Group), Review of Particle Physics, *Phys. Rev.* **D98**, 030001 (2018).
- [57] J. Erler and M. Schott, Electroweak Precision Tests of the Standard Model after the Discovery of the Higgs Boson, *Prog. Part. Nucl. Phys.* **106**, 68 (2019), arXiv:1902.05142 [hep-ph].
- [58] P. A. Zyla *et al.* (Particle Data Group), Review of Particle Physics, *PTEP* **2020**, 083C01 (2020).
- [59] S. Borsanyi *et al.* (Budapest-Marseille-Wuppertal), Hadronic vacuum polarization contribution to the anomalous magnetic moments of leptons from first principles, *Phys. Rev. Lett.* **121**, 022002 (2018), arXiv:1711.04980 [hep-lat].
- [60] B. Colquhoun, R. J. Dowdall, C. T. H. Davies, K. Hornbostel, and G. P. Lepage, Υ and Υ' Leptonic Widths, a_μ^b and m_b from full lattice QCD, *Phys. Rev. D* **91**, 074514 (2015), arXiv:1408.5768 [hep-lat].
- [61] A. Blondel, J. Gluza, S. Jadach, P. Janot, and T. Riemann, eds., *Theory for the FCC-ee: Report on the 11th FCC-ee Workshop Theory and Experiments*, CERN Yellow Reports: Monographs, Vol. 3/2020 (CERN, Geneva, 2019) arXiv:1905.05078 [hep-ph].
- [62] Combination of CDF and D0 results on the mass of the top quark using up 9.7fb^{-1} at the Tevatron (2016), arXiv:1608.01881 [hep-ex].
- [63] A. M. Sirunyan *et al.* (CMS), Measurement of the top quark mass using single top quark events in proton-proton collisions at $\sqrt{s} = 8$ TeV, *Eur. Phys. J. C* **77**, 354 (2017), arXiv:1703.02530 [hep-ex].
- [64] M. Aaboud *et al.* (ATLAS), Measurement of the Higgs boson mass in the $H \rightarrow ZZ^* \rightarrow 4\ell$ and $H \rightarrow \gamma\gamma$ channels with $\sqrt{s} = 13$ TeV pp collisions using the ATLAS detector, *Phys. Lett. B* **784**, 345 (2018), arXiv:1806.00242 [hep-ex].
- [65] Measurement of the Higgs boson mass in the $H \rightarrow ZZ^* \rightarrow 4\ell$ decay channel with $\sqrt{s} = 13$ TeV pp collisions using the ATLAS detector at the LHC (2020).
- [66] A. M. Sirunyan *et al.* (CMS), Measurements of properties of the Higgs boson decaying into the four-lepton final state in pp collisions at $\sqrt{s} = 13$ TeV, *JHEP* **11**, 047, arXiv:1706.09936 [hep-ex].
- [67] A. M. Sirunyan *et al.* (CMS), A measurement of the Higgs boson mass in the diphoton decay channel, *Phys. Lett. B* **805**, 135425 (2020), arXiv:2002.06398 [hep-ex].
- [68] R. Aaij *et al.* (LHCb), Measurement of the W boson mass (2021), arXiv:2109.01113 [hep-ex].
- [69] T. A. Aaltonen *et al.* (CDF, D0), Tevatron Run II combination of the effective leptonic electroweak mixing angle, *Phys. Rev. D* **97**, 112007 (2018), arXiv:1801.06283 [hep-ex].
- [70] P. Janot and S. Jadach, Improved Bhabha cross section at LEP and the number of light neutrino species, *Phys. Lett. B* **803**, 135319 (2020), arXiv:1912.02067 [hep-ph].
- [71] W. Bernreuther, L. Chen, O. Dekkers, T. Gehrmann, and D. Heisler, The forward-backward asymmetry for massive bottom quarks at the Z peak at next-to-next-to-leading order QCD, *JHEP* **01**, 053, arXiv:1611.07942 [hep-ph].
- [72] K. Abe *et al.* (SLD), First direct measurement of the parity violating coupling of the Z_0 to the s quark, *Phys. Rev. Lett.* **85**, 5059 (2000), arXiv:hep-ex/0006019.
- [73] A. Keshavarzi, W. J. Marciano, M. Passera, and A. Sirlin, Muon $g - 2$ and $\Delta\alpha$ connection, *Phys. Rev. D* **102**, 033002 (2020), arXiv:2006.12666 [hep-ph].
- [74] H. Flacher, M. Goebel, J. Haller, A. Hocker, K. Monig, *et al.*, Revisiting the global electroweak fit of the standard model and beyond with Gfitter, *Eur.Phys.J.* **C60**, 543 (2009), arXiv:0811.0009 [hep-ph].
- [75] S. Borsanyi *et al.*, Leading hadronic contribution to the muon magnetic moment from lattice QCD, *Nature* **593**, 51 (2021), arXiv:2002.12347 [hep-lat].
- [76] D. Buttazzo, G. Degrossi, P. P. Giardino, G. F. Giudice, F. Sala, A. Salvio, and A. Strumia, Investigating the near-criticality of the Higgs boson, *JHEP* **12**, 089, arXiv:1307.3536 [hep-ph].